International Journal of Mathematical Archive-8(6), 2017, 153-166
Available online through www.ijma.info ISSN 2229 – 5046

MAGNETO HYDRODYNAMIC EFFECTS ON NON-NEWTONIAN EYRING-POWELL FLUID FROM A CIRCULAR CYLINDER WITH SORET AND DUFOUR EFFECTS

L. NAGARAJA[1,2], M. SUDHAKAR REDDY[2*], M. SURYANARAYANA REDDY[3]

**[1]Research Scholar, Department of Mathematics,
Madanapalle Institute of technology & Science,
Madanaoalle, Andhra Pradesh, India.**

**[2*]Department of Mathematics,
Madanapalle Institute of Technology and Science,
Madanapalle, Andhra Pradesh, India.**

**[3]Assistant Professor, Department of Mathematics,
JNTUA College of Engineering, Pulivendula, Andhra Pradesh, India.**

Received On: 22-05-17; Revised & Accepted On: 22-06-17)

ABSTRACT

P*resent study offered for the laminar free convection boundary layer flow of Eyring-powell non-Newtonian fluid past a horizontal circular cylinder in the occurrence of magnetic effect, and Soret, Dufour effects. The cylinder surface is maintained at non-uniform surface temperature. The boundary layer conservation equations, transformed into non-dimensional form via appropriate non-similarity variables, and the emerging boundary value problem is solved computationally with the second order accurate implicit Keller-Box finite difference scheme. Evaluation on velocity, temperature and concentration are illustrated graphically. Skin friction and Nusselt number are presented tabular form.*

Key Words: *Eyring-Powell model, porous medium, MHD; heat transfer, Skin friction, Nusselt number, Soret and Dufour effects.*

NOMENCLATURE

C_f	skin friction coefficient
f	non-dimensional steam function
Gr	Grashof number
g	acceleration due to gravity
Sr	Soret effect
Du	Dufour effect
k	thermal conductivity of fluid
Nu	local Nusselt number
Pr	prandtl number
Sc	schmidt number
T	temperature of the fluid
u, v	non-dimensional velocity components along the x- and y- directions, respectively
V	velocity vector x stream wise coordinate y transverse coordinate

Corresponding Author: M. Sudhakar Reddy*[2]
[2*]Department of Mathematics, Madanapalle Institute of Technology and Science, Madanapalle, Andhra Pradesh, India.

GREEK SYMBOLS

α	thermal diffusivity
β	fluid parameter
δ	local non-Newtonian parameter
η	dimensionless radial coordinate
μ	dynamic viscosity
ν	kinematic viscosity
θ	dimensionless temperature
ρ	density of non-Newtonian fluid
ξ	dimensionless tangential coordinate
ψ	dimensionless stream function
ε	fluid parameter

SUBSCRIPTS

W	condition at the wall
∞	free stream condition

1. INTRODUCTION

Many modern engineering tenders involve the study of non-Newtonian fluids. These include petroleum drilling muds [1], biological gels [2], polymer processing [3] and food processing [4]. Most commonly, the viscosity of non-Newtonian fluids is dependent on shear rate. Some non-Newtonian fluids with shear-independent viscosity, however, still exhibit normal stress difference or other non-Newtonian behavior. Several salt solutions and molten polymers are non-Newtonian fluids, as are many other liquids encountered in science and technology such as dental creams, physiological fluids, detergents and paints. In a non-Newtonian fluid, the relation between the shear stress and the shear rate is generally non-linear and can even be time-dependent. Recently Malik *et al.* [5] studied mixed convection floe of MHD Eyring-Powell fluid over a stretching sheet a numerical study. They found that rate of heat and mass transfer decreases for all parameters. Abdul Gafar *et al.* [6] studied computational study of non-Newtonian Eyring-Powell fluid from a horizontal circular cylinder with biot number effect. Discussed filled presence of porous media under the effect of radiation and MHD [7-8], Abdul Hakeem *et al.* [9] studied Heat transfer of Darcy MHD flow of Nano-fluid over a stretching/shrinking surface. They found that Nano fluid velocity, temperature, skin friction coefficient and reduced Nusselt number are discussed. Animasaun Raju *et al.* [10] studied Unequal diffusivities case of homogeneous–heterogeneous reactions within viscoelastic fluid flow in the presence of induced magnetic-field and nonlinear thermal radiation. They found induced magnetic field effect on viscoelastic fluid flow past a stretching sheet in the presence of nonlinear thermal radiation and homogeneous–heterogeneous reactions. Recently, Subba Rao *et.al.* [11] Studied the Boundary Layer Flows of non-Newtonian fluid from an inclined vertical plate in the presence of hydrodynamic and thermal slip conditions using the Keller Box finite difference method.

A number of theoritical and computational studies have been communicated on transport phenomena from cylindrical bodies, which frequently arise in polymer processing system. These Newtonian studies were focused more on heat transfer aspects and include Eswara , Nath,[24] and Rotte, Beek,[25] and the pioneering analysis of Sakiadis *et. al.* [26]. Further more recent studies examining multi-physical and chemical transport from cylindrical bodies included Zueco *et al.* [27]-[28]. An early investigation of rheological boundary layer heat transfer from horizontal cylinder was presented by Chen and Leonard [40], who consider the power-law model and demonstrated that the transverse curvature has a strong effect on skin friction at moderate and large distance from the leading edge of the boundary layer. Lin and Chen also studied axisymmetric laminar boundary layer convection flow of a power-law non-Newtonian over both circular cylinder and spherical body using the Merk-Chao series solution method.

In many chemical engineering and nuclear process systems, curvature of the vessels employed is a critical aspect of optimizing thermal performance. Examples of curved bodies featuring in process systems include torus geometries, wavy surfaces, cylinders, cones, ellipses, oblate spheroids and in particular, spherical geometries, the latter being very popular for storage of chemicals and also batch reactor processing. Heat transfer from spheres has therefore mobilized much attention among chemical engineering researchers who have conducted both experimental and computational investigations for both Newtonian and non-Newtonian fluids. Beg *et al.*, [41] examined the free convection magneto hydrodynamic flow from a sphere in porous media using network simulation, showing that temperatures are boosted with magnetic field and heat transfer is enhanced from the lower stagnation point towards the upper stagnation point.

The objective of the present work, a mathematical model is developed for steady, natural convection boundary layer flow in a Eyring-Powell non-Newtonian fluid past a circular cylinder maintained at non-uniform surface temperature. A finite difference numerical solution is obtained for the transformed nonlinear two-point boundary value problem subject to physically appropriate boundary conditions at the cylinder surface and in the free stream. The impact of the emerging thermo-physical parameters i.e. Eyring-Powell fluid parameter (ε), the local non-Newtonian parameter (δ), Prandtl number (Pr), dimensionless tangential coordinate (ξ) magnetic parameter (M) Schmidt number (Sc) and temperature evaluation on velocity, temperature, skin friction and Nusselt number are illustrated graphically and in Tables. Validation of solutions with earlier published work is included. Detailed evaluation of the physics is included.

2. MATHEMATICAL MODEL

Steady, laminar, two-dimensional boundary layer flows and heat transfer of a viscous incompressible Eyring-Powell fluid over a circular cylinder is considered, as illustrated in Fig. 1. The x-coordinate (tangential) is measured along the circumference of the horizontal cylinder from the lowest point and the y-coordinate (radial) is directed perpendicular to the surface, with a denoting the radius of the horizontal cylinder. $\Phi = x/a$ Is the angle of the y-axis with respect to the vertical $0 \le \Phi \le \pi$. The gravitational acceleration **g**, acts downwards. We also assume that the Boussineq approximation holds i.e. that density variation is only experienced in the buoyancy term in the momentum equation. Both horizontal cylinder and Eyring-Powell fluid are maintained initially at the same temperature. Instantaneously they are raised to a temperature $T_W > T_\infty$, the ambient temperature of the fluid which remains unchanged. In line with the approach of Yih [24] and introducing the boundary layer estimates, the governing equations can be written as:

$$\frac{\partial u}{\partial x}+\frac{\partial v}{\partial y}=0 \tag{1}$$

$$u\frac{\partial u}{\partial x}+v\frac{\partial u}{\partial y}=\left(\nu+\frac{1}{\rho\beta c}\right)\frac{\partial^2 u}{\partial y^2}-\frac{1}{2\rho\beta c^3}\left(\frac{\partial u}{\partial y}\right)^2\frac{\partial^2 u}{\partial y^2}-\frac{\sigma B_0^2}{\rho}u+g\beta(T-T_\infty)\sin\left(\frac{x}{a}\right)+g\beta^*(c-c_\infty)\sin\left(\frac{x}{a}\right) \tag{2}$$

$$u\frac{\partial T}{\partial x}+v\frac{\partial T}{\partial y}=\alpha\frac{\partial^2 T}{\partial y^2}+\frac{D_M K_T}{c_S c_P}\frac{\partial^2 C}{\partial y^2} \tag{3}$$

$$u\frac{\partial C}{\partial x}+v\frac{\partial C}{\partial y}=D_M\frac{\partial^2 C}{\partial y^2}+\frac{D_M K_T}{T_M}\frac{\partial^2 T}{\partial y^2} \tag{4}$$

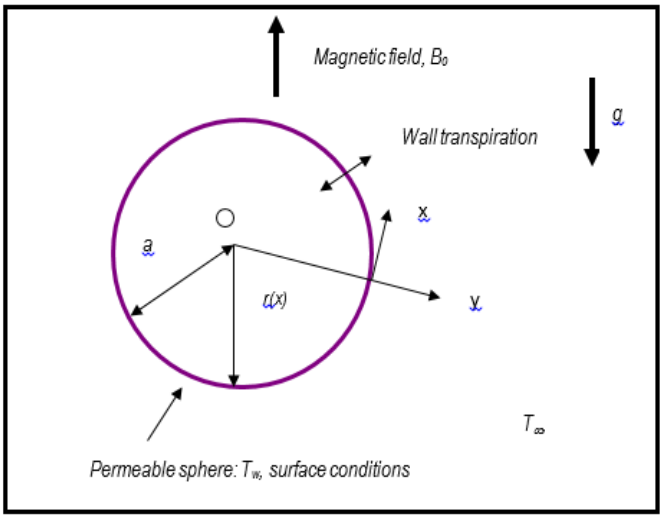

Figure 1: Physical Model and Coordinate System

Anywhere u and v are the velocity components in the x - and y -directions respectively, ν -the kinematic viscosity of the conducting fluid, β -is the non-Newtonian Eyring parameter, α -the thermal diffusivity, T -the temperature, K -the permeability coefficient of the porous medium, T_∞ -the free stream temperature. The boundary conditions are arranged at the circulation and the edge of the boundary layer regime, respectively as follows:

$$\begin{aligned} &u=u_w, v=-v_w, T=T_w &&: As \quad y=0 \\ &u\to 0, T\to T_\infty &&: At \quad y\to\infty \end{aligned} \tag{5}$$

Where the stream function ψ is defined by $u = \partial\psi/\partial y$ and $u = -\partial\psi/\partial x$, and therefore, the continuity equation is automatically satisfied. In order to write the governing equations and the boundary conditions in dimensionless form, the following non-dimensional quantities are introduced:

$$\left\{\begin{array}{l} \xi = \dfrac{x}{a}, \qquad \eta = \dfrac{y}{a}Gr^{1/4}, \qquad \psi = \nu\xi Gr^{1/4} f \\ \theta = \dfrac{T-T_\infty}{T_w-T_\infty}, \phi = \dfrac{C-C_\infty}{C_w-C_\infty}, q_r = \dfrac{-16\sigma^* T_\infty^3}{3K^*}\dfrac{\partial T}{\partial y} \end{array}\right\} \tag{6}$$

In view of non-dimensional quantities (6), Equations (1)-(4) reduce to the following coupled, nonlinear, dimensionless partial differential equations for momentum and energy for the region,

$$(1+\varepsilon) f''' - f'^2 + ff'' - \varepsilon\delta\xi^2 f''^2 f''' - Mf' + \frac{\sin\xi}{\xi}(\theta + N\phi) = \xi\left(f'\frac{\partial f'}{\partial\xi} - f''\frac{\partial f}{\partial\xi}\right) \tag{7}$$

$$\frac{1}{\Pr}\theta'' + Du\phi'' + f\theta' = \xi\left(f'\frac{\partial\theta}{\partial\xi} - \theta'\frac{\partial f}{\partial\xi}\right) \tag{8}$$

$$\frac{1}{Sc}\phi'' + Sr\theta'' + f\phi' = \xi\left(f'\frac{\partial\phi}{\partial\xi} - \phi'\frac{\partial f}{\partial\xi}\right) \tag{9}$$

The transformed dimensionless boundary conditions are

$$\begin{array}{llll} At & \eta = 0, & f = 0, \quad f' = 0, & \theta = 1 \\ As & \eta \to \infty & f' \to 0 & \theta \to 0 \end{array} \tag{10}$$

In the above equations, the primes denote the differentiation with respect to η, the dimensionless radial coordinate, and ξ is the dimensionless tangential coordinate, $Da = K/a^2 Gr^{1/2}$ is the Darcy parameter and $Gr = g\beta(T_w - T_\infty)a^3/\nu^3$ is the Grashof (free convection) parameter. $\Pr = \nu/\alpha$ is the Prandtl number, $Sc = Dm/\nu$ is Schmidt number, $\varepsilon = 1/\nu\beta\rho c$ is Eyring-Powell fluid parameter, $\delta = \nu^2 Gr^{3/2}/2c^2 a^4$, $M = \sigma B_0^2 a^2/\rho\nu Gr^{1/2}$ is magnetic parameter, $Gr = \dfrac{g\beta(T_w - T_\infty)a^3}{\nu^3}$ is the Grashof number, $Du = \dfrac{D_M K_T}{\nu c_S c_P}\dfrac{C_w - C_\infty}{T_w - T_\infty}$ and $Sr = \dfrac{D_M K_T}{\nu T_M}\dfrac{T_w - T_\infty}{C_w - C_\infty}$ are Sort and Dufour coefficients. The engineering design quantities of physical interest include the skin-friction coefficient and Nusselt number, are given as,

$$C_f Gr^{-3/4} = (1+\varepsilon)\xi f''(0) - \frac{\delta}{3}\varepsilon\xi^3 (f''(\xi,0))^3 \tag{11}$$

$$\frac{Nu}{\sqrt[4]{Gr}} = -\theta'(0) \tag{12}$$

3. NUMERICAL SOLUTIONS

The Keller-Box implicit difference method is implemented to solve the nonlinear boundary value problem defined by equations (6) -(7) with boundary conditions (8). This technique, despite recent developments in other numerical methods, remains a powerful and very accurate approach for parabolic boundary layer flows. It is unconditionally stable and achieves exceptional accuracy (12). Recently this method has been deployed in resolving many challenging, multi-physical fluid dynamics problems. These include hydro magnetic Sakiadis flow of non-Newtonian fluids (13), Nano-fluid transport from a stretching sheet (14), radiate rheological magnetic heat transfer (15), water hammer modeling (16), porous media convection (17) and magnetized viscoelastic stagnation flow (18). The Keller-Box discretization is fully coupled at each step which reflects the physics of parabolic systems-which are also fully coupled. Discrete calculus associated with the Keller-Box scheme has also been shown to the fundamentally different from all other mimetic (physics capturing) numerical methods, as elaborated by Keller (12). The key stages involved are as follows:

a. Reduction of the Nth order partial differential equation system to N first order equation
b. Finite difference discretization of reduced equation
c. Quasilinearization of nonlinear Keller algebraic equations
d. Block-tridiagonal elimination of linearized Keller algebraic equations

Stage (a): Decomposition of Nth order partial differential equation system to N first order equations:

Equations (6)-(7) subject to the boundary conditions (8) are first cast as a multiple system of first order differential equations. New dependent variables are introduced:

$$u(x,y) = f', v(x,y) = f'', s(x,y) = \theta, t(x,y) = \theta' \tag{13}$$

These denote the variables for velocity, temperature respectively. Now equations (6)-(7) are solved as a set of fifth order simultaneous differential equations:

$$f' = u \tag{14}$$

$$u' = v \tag{15}$$

$$s' = t \tag{16}$$

$$g' = p \tag{16}$$

$$(1+\varepsilon)v' - u^2 + fv - \varepsilon\delta\xi^2 v^2 v' - \left(M + \frac{1}{DaGr^{1/2}}\right)u + \frac{\sin\xi}{\xi}(\theta + N\phi) = \xi\left(u\frac{\partial u}{\partial \xi} - v\frac{\partial f}{\partial \xi}\right) \tag{17}$$

$$\frac{1}{\Pr}t' + Du\phi'' + ft' = \xi\left(u\frac{\partial s}{\partial \xi} - t\frac{\partial f}{\partial \xi}\right) \tag{18}$$

$$\frac{1}{Sc}\phi'' + Sr\theta'' + f\phi' = \xi\left(f'\frac{\partial \phi}{\partial \xi} - \phi'\frac{\partial f}{\partial \xi}\right) \tag{19}$$

Where the primes denote differentiation w.r.t variable η. In terms of the dependent variables, the boundary conditions assume the form:

$$\begin{aligned} &At \quad \eta = 0, \qquad f = 0, \quad f' = 0, \qquad \theta = 1 \\ &As \quad \eta \to \infty \qquad f' \to 0 \quad \theta \to 0 \end{aligned} \tag{20}$$

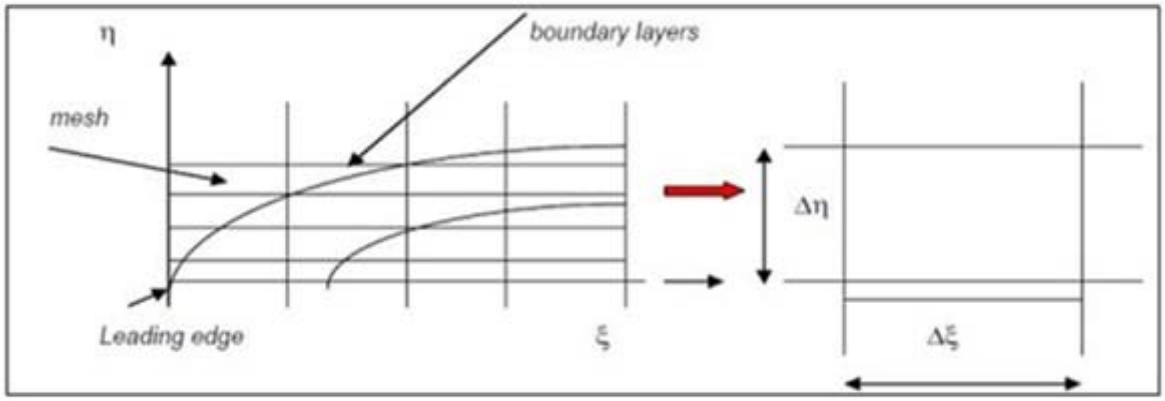

Figure-2: Keller box computational domain

Stage (b): Finite Difference Discretization

$$\eta_0 = \eta_{j-1} + h_j, \quad j = 1,2,3,...,J, \qquad \eta_j = \eta_\infty \tag{21}$$

$$\xi^0 = 0, \quad \xi^n = \xi^{n-1} + k_n \qquad n = 1,2,3,...,N \tag{22}$$

$$g_{j-1/2}^{n-1/2} = \frac{1}{4}(g_j^n + g_{j-1}^n + g_j^{n-1} + g_{j-1}^{n-1}), \tag{23}$$

$$\left(\frac{\partial g}{\partial \eta}\right)_{j-1/2}^{n-1/2} = \frac{1}{2h_j}(g_j^n - g_{j-1}^n + g_j^{n-1} - g_{j-1}^{n-1}), \tag{24}$$

$$\left(\frac{\partial g}{\partial \xi}\right)_{j-1/2}^{n-1/2} = \frac{1}{2k^n}(g_j^n - g_{j-1}^n + g_j^{n-1} - g_{j-1}^{n-1}), \tag{25}$$

$$h_j^{-1}(f_j^n - f_{j-1}^n) = u_{j-1/2}^n, \tag{26}$$

$$h_j^{-1}(u_j^n - u_{j-1}^n) = v_{j-1/2}^n, \tag{27}$$

$$h_j^{-1}(s_j^n - s_{j-1}^n) = t_{j-1/2}^n, \tag{28}$$

$$h_j^{-1}(g_j^n - g_{j-1}^n) = p_{j-1/2}^n,$$

$$(1+\varepsilon)(v_j - v_{j-1}) - (1+\alpha)\frac{h_j}{4}(u_j + u_{j-1})^2 + (1+\alpha)\frac{h_j}{4}(f_j + j_{j-1})(v_j + v_{j-1})$$

$$+\frac{\sin\xi}{\xi}\frac{h_j}{2}(s_j + s_{j-1}) - \xi^2\frac{\varepsilon\delta}{4}(v_j - v_{j-1})(v_j + v_{j-1})^2 - \left(M + \frac{1}{DaGr^{1/2}}\right)\frac{h_j}{2}(u_j + u_{j-1})$$

$$-\frac{\alpha h_j}{2}f_{j-1/2}^{n-1}(v_j + v_{j-1}) + \frac{\alpha h_j}{2}v_{j-1/2}^{n-1}(f_j + f_{j-1}) = [R_1]_{j-1/2}^{n-1}$$

(29)

$$\frac{1}{\Pr}(t_j - t_{j-1}) + Du(p_j - p_{j-1}) + (1+\alpha+\xi\cot\xi)\frac{h_j}{4}(t_j + t_{j-1})(f_j + f_{j-1})$$

$$-\frac{\alpha h_j}{4}(u_j + u_{j-1})(s_j + s_{j-1}) + \frac{\alpha h_j}{2}s_{j-1/2}^{n-1}(u_j + u_{j-1}) - \frac{\alpha h_j}{2}u_{j-1/2}^{n-1}(s_j + s_{j-1})$$

$$-\frac{\alpha h_j}{2}f_{j-1/2}^{n-1}(t_j + t_{j-1}) + \frac{\alpha h_j}{2}t_{j-1/2}^{n-1}(f_j + f_{j-1}) = [R_2]_{j-1/2}^{n-1} \tag{30}$$

$$\alpha = \frac{\xi^{n-1/2}}{k_n}, B = \frac{\sin(\xi^{n-1/2})}{\xi^{n-1/2}} \tag{31}$$

$$f_0^n = u_0^n = 0, \quad s_0^n = 1, \ v_j^n = 0, \quad s_j^n = 0 \tag{32}$$

$$[R_1]_{j-1/2}^{n-1} = h_j\begin{pmatrix}(1+\varepsilon)(v')_{j-1/2}^{n-1} - (1-\alpha)(u^2)_{j-1/2}^{n-1} + (1-\alpha)f_{j-1/2}^{n-1}v_{j-1/2}^{n-1} - \varepsilon\delta\xi^2(v^2)_{j-1/2}^{n-1}(v')_{j-1/2}^{n-1} \\ -(M + \frac{1}{DaGr^{1/2}})u_{j-1/2}^{n-1} + \frac{\sin\xi}{\xi}s_{j-1/2}^{n-1}\end{pmatrix} \tag{33}$$

$$[R_2]_{j-1/2}^{n-1} = h_j\left(\frac{1}{\Pr}(1+\frac{4}{3}k)(t')_{j-1/2}^{n-1} + (1-\alpha)f_{j-1/2}^{n-1}t_{j-1/2}^{n-1} + \alpha u_{j-1/2}^{n-1}s_{j-1/2}^{n-1}\right) \tag{34}$$

The boundary conditions are:

$$f_0^n = u_0^n = 0, \quad s_0^n = 1, \ v_j^n = 0, \quad s_j^n = 0 \tag{35}$$

Stage (c): Quasilinearization of Non-linear Keller Algebraic Equations

Assuming $f_j^{n-1}, u_j^{n-1}, v_j^{n-1}, s_j^{n-1}, t_j^{n-1}$ to be known for $0 \le j \le J$, then equations (12)-(16) constitute a system of 7J+7 equations for the solutions of 7J+7 unknowns $f_{j,}^n, u_j^n, v_j^n, s_j^n, t_j^n, \ j = 0,1,2,...,J$. This non-linear system of algebraic equations is linearized by means of Newtonian's method as explained in [19-20, 29-39]

Stage (d): Block-tridiagonal Elimination solution of linear Keller Algebraic Equations

The linearized system is solved by the block-elimination method, since it possesses a block-tridiagonal structure. The bock-tridiagonal structure generated consists of block matrices. The complete linearized system is formulated as a block matrix system, where each element in the coefficient matrix is a matrix itself, and this system is solved using the efficient Keller-box method. The numerical results are strongly influenced by the number of mesh points in both

directions. After some trials in the η-direction (radial coordinate) a larger number of mesh points are selected whereas in the ξ direction (tangential coordinate) significantly less mesh points are utilized. η_{max} has been set at 25 and this defines an adequately large value at which the prescribed boundary conditions are satisfied. ξ maxis set at 3.0 for this flow domain. Mesh independence is achieved in the present computations. The numerical algorithm is executed in **MATLAB** on a PC. The method demonstrates excellent stability, convergence and consistency, as elaborated by Keller [20]

4. RESULT & DISCUSSIONS

In this section, the influence of various physical parameters like Eyring-Powell fluid parameters (ε, δ), magnetic parameter (M), radiation parameter (R), Prandlt number (Pr),Schmidt number (Sc), and buoyancy ratio (N) on velocity profiles $f'(\eta)$, temperature profiles $\theta(\eta)$ and concentration profiles $\phi(\eta)$ have been analyzed.

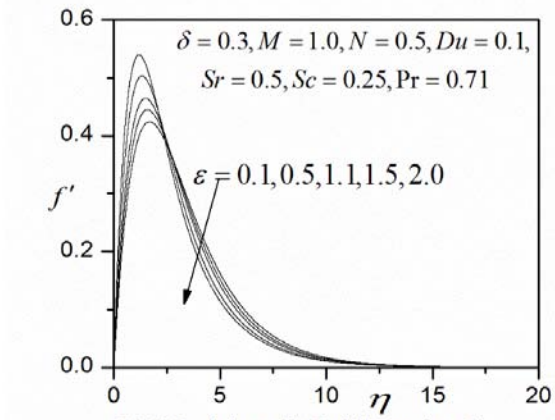

Fig.3(a). velocity profiles for different values of ε

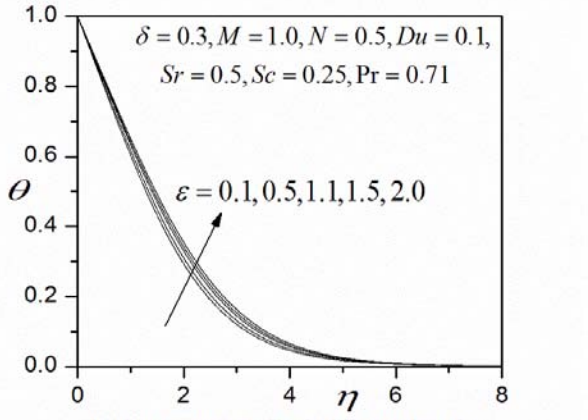

Fig.3(b). temperature profiles for different values of ε

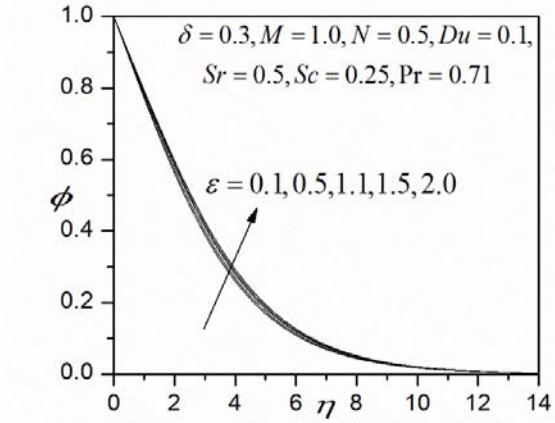

Fig.3(c). concentration profiles for different values of ε

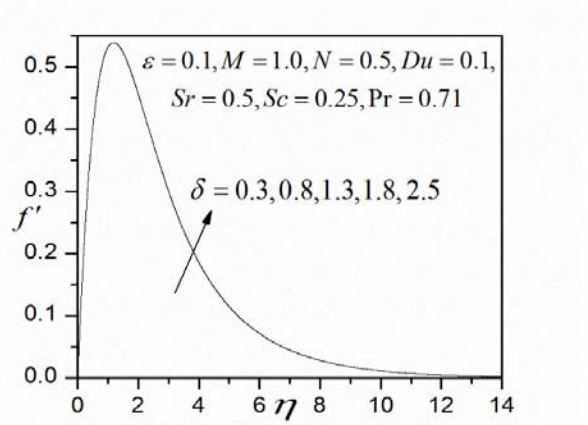

Fig.4(a). velocity profiles for different values of δ

Table 1&2 Document results for the influence of the Prandlt number (Pr) and the Magnetic parameter (M) on skin friction $(-f''(0))$ heat transfer rate $(-\theta(0))$ and Sharehood number $(-\phi'(0))$. It has been observed that increasing Pr reduces skin friction and Sharehood number but increases heat transfer rate (Nusselt numbers). Also, increasing M is found to decrease both the skin friction and heat transfer rate (Nusselt number) and Sharehood number.

Table 3 Shows that the comparisons of the various values of ξ. In order to verify the accuracy of our present method, we have compared our results with those of Merkin [25] and Yih [26]

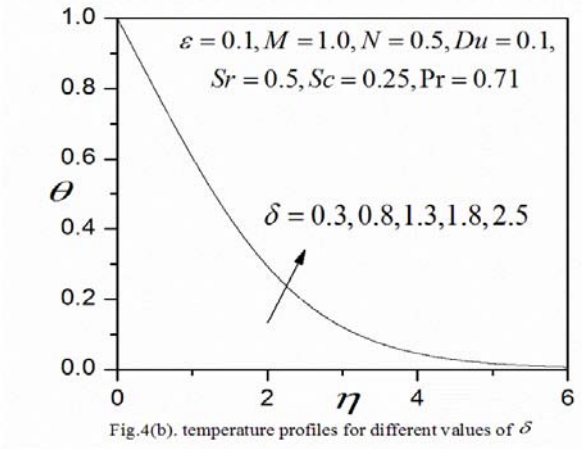

Fig.4(b). temperature profiles for different values of δ

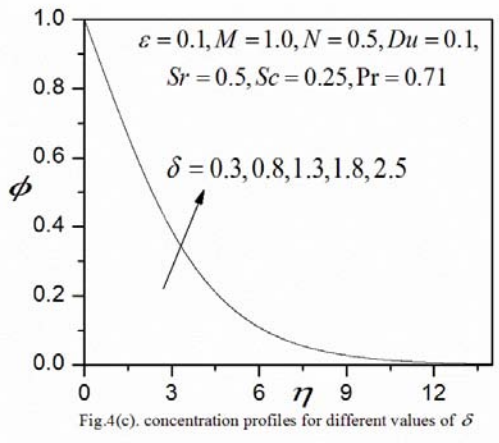

Fig.4(c). concentration profiles for different values of δ

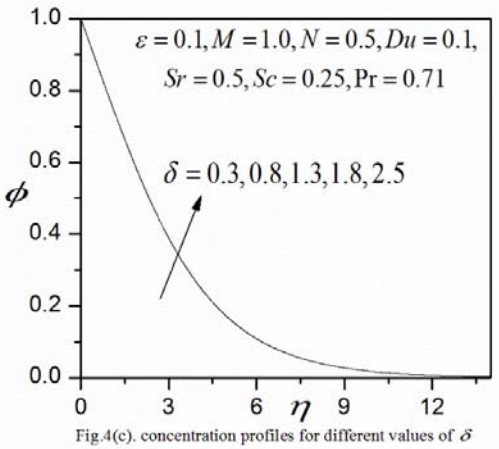

Fig.4(c). concentration profiles for different values of δ

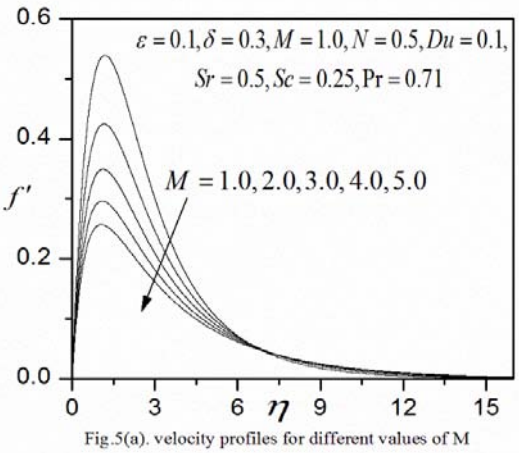

Fig.5(a). velocity profiles for different values of M

Figures 3(a)-3(c) illustrates the effect of Eyring-Powell fluid parameter ε, on the velocity $f'(\eta)$, temperature $\theta(\eta)$ and concentration $\phi(\eta)$ distributions through the boundary layer regime. Velocity is significantly decreased with increasing at larger distance from the cylinder surface owing to the simultaneous drop in dynamic viscosity. Conversely temperature and concentration are consistently enhanced with increasing values of ε. The mathematical model reduces to the Newtonian viscous flow model as $\varepsilon \to 0$ and $\delta \to 0$. In fig. 3b temperatures are clearly minimized for the Newtonian case (ε =0) and maximized for the strongest non-Newtonian case (ε =2.0).

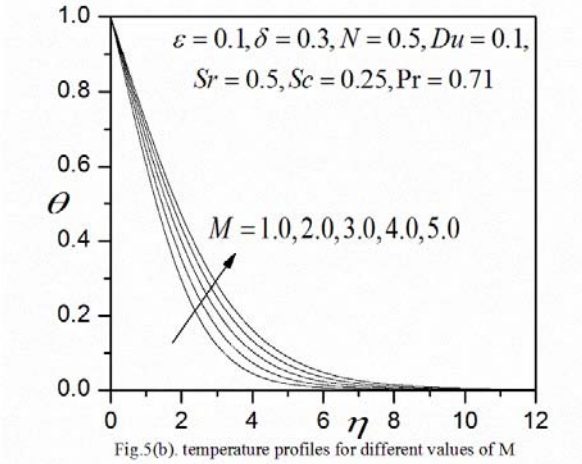

Fig.5(b). temperature profiles for different values of M

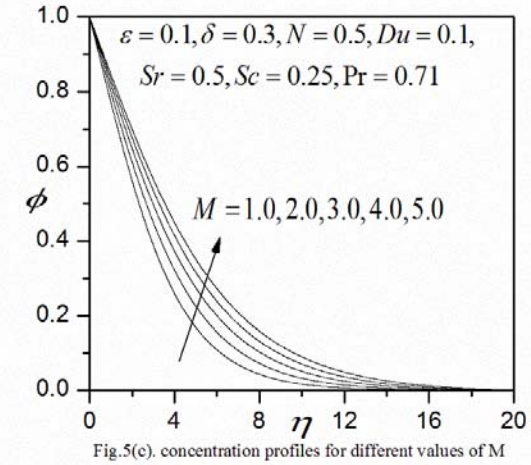

Fig.5(c). concentration profiles for different values of M

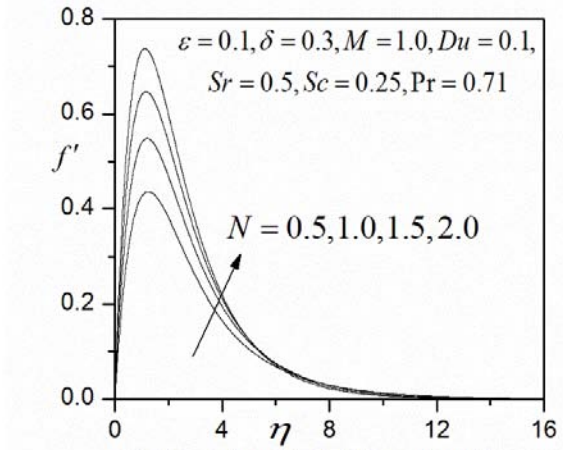

Fig.6(a). velocity profiles for different values of N

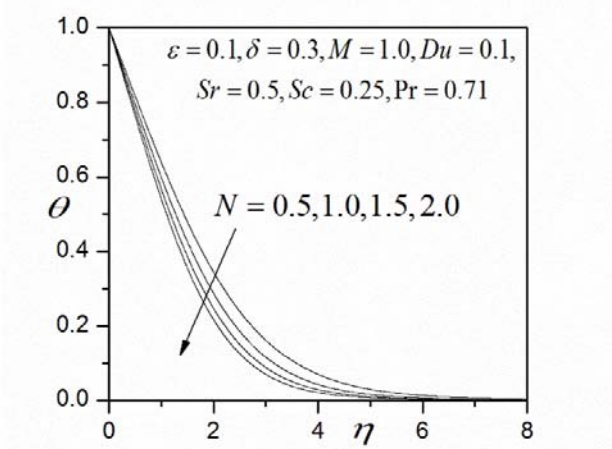

Fig.6(b). temperature profiles for different values of N

Figures 4(a)-4(c) depict the velocity $f'(\eta)$, temperature $\theta(\eta)$ and concentration $\phi(\eta)$ distributions with increasing local non-Newtonian parameter δ. Very little tangible effect is observed in fig. 4a, although there is a very slight increase in velocity with increase in δ. Similarly, there is only a very slight depression in temperature, concentration magnitudes in Fig.4(b), (c) with a rise in δ

Figures 5(a)-5(c) the dimensionless velocity $f'(\eta)$, temperature $\theta(\eta)$ and concentration $\phi(\eta)$ for various values of magnetic parameter M are shown. Fig. 5(a) represents the velocity profile for

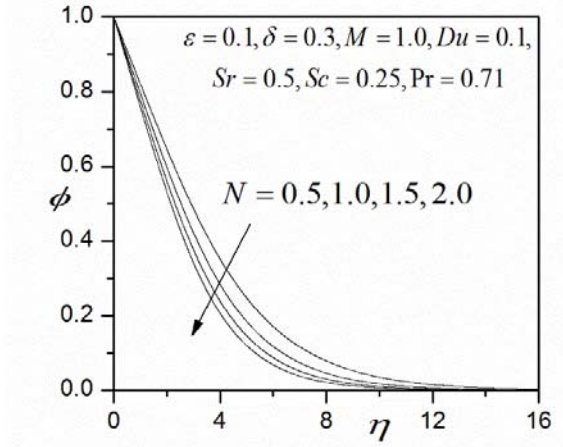

Fig.6(c). concentration profiles for different values of N

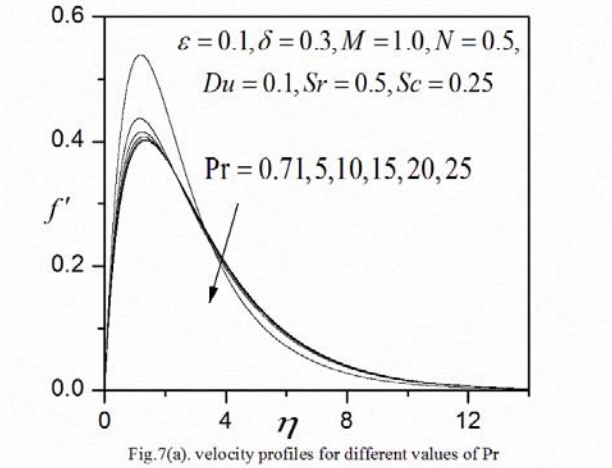

Fig.7(a). velocity profiles for different values of Pr

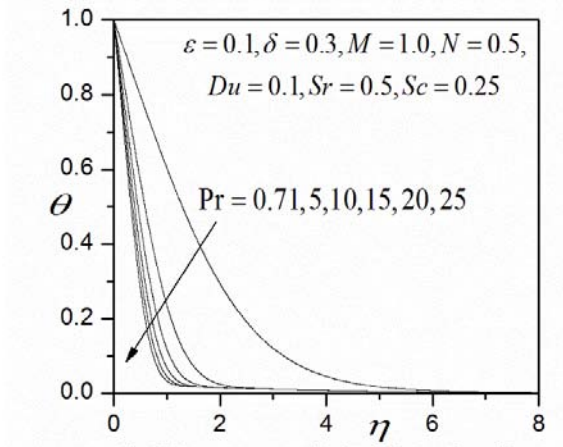

Fig.7(b). temperature profiles for different values of Pr

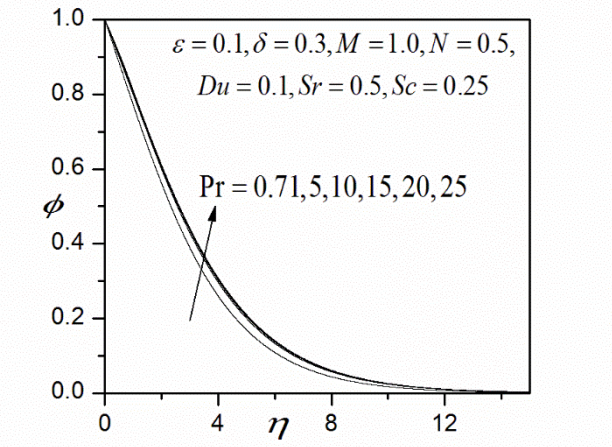

Fig.7(c). concentration profiles for different values of Pr

the different values of magnetic field parameter M. It is observed that velocity of the flow decreases significantly throughout the fluid domain with increasing values of magnetic parameter M. Application of a magnetic field to an electrically conducting fluid produces a kind of drag-like force called Lorentz force. This force causes reduction in the fluid velocity within the boundary layer as the magnetic field opposes the transport phenomena. In Fig. 5(b), the

temperature distribution increases with increasing magnetic values. The effect of Lorentz force on velocity profiles generated a kind of friction on the flow this friction in turn generated more heat energy which eventually increases the temperature distribution in the flow (see Fig. 5(b)). The concentration profile for the fluid has significant increase with increase in the magnetic parameter due to the temperature gradient inherent in the viscosity of the fluid as shown in Fig. 5(c).

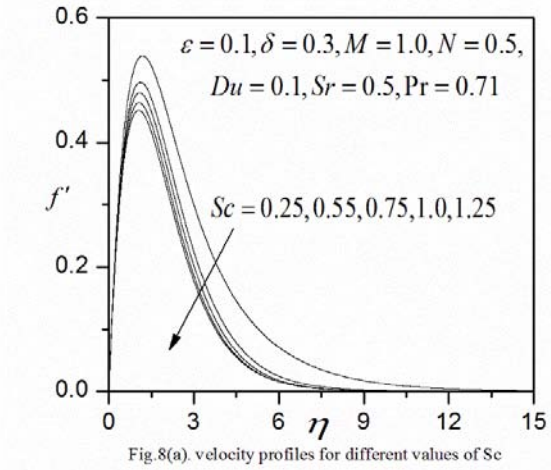

Fig.8(a). velocity profiles for different values of Sc

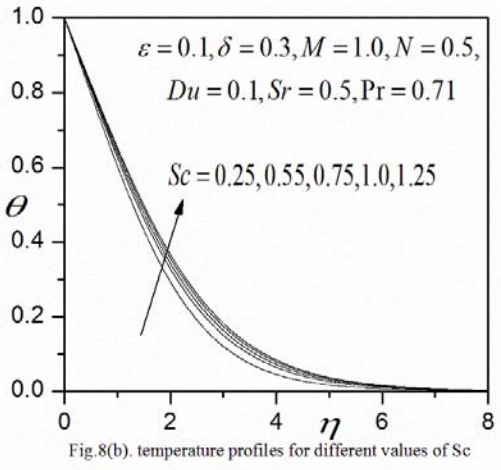

Fig.8(b). temperature profiles for different values of Sc

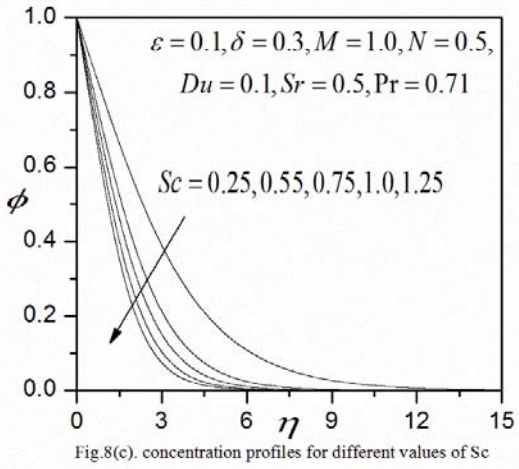

Fig.8(c). concentration profiles for different values of Sc

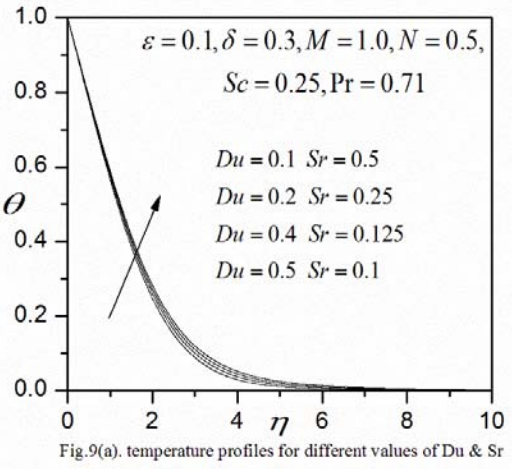

Fig.9(a). temperature profiles for different values of Du & Sr

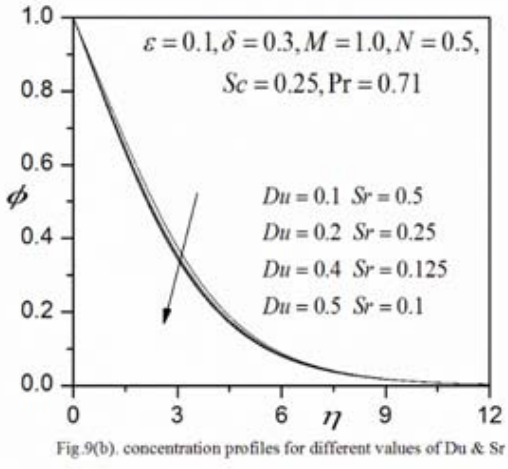

Fig.9(b). concentration profiles for different values of Du & Sr

Figures 6(a)-6(c) depict the velocity $f'(\eta)$, temperature $\theta(\eta)$ and concentration $\phi(\eta)$ distributions, rise in *N* clearly induces an increase in velocity as seen in Figure 6(a), the flow is significantly accelerated for *N* = 2.0, where once again a velocity overshoot is computed at intermediate distance from the cylinder ($\eta \sim 3$). For *N* = 0.5, 1.0, 1.5, 2.0, no velocity overshoot is apparent although velocities are increased in the regime continuously. In Figure 6(b) for positive *N* (thermal and concentration buoyancy forces assisting each other), this trend is reversed with a decrease in

temperature *i.e.* cooling of the boundary layer regime. In Figure 6(c), a similar response for the concentration distribution is observed as in the case of the temperature distribution, with ϕ values increasing fractionally with positive N values. Opposing buoyancy forces ($N < 0$) therefore enhance species diffusion in the regime whereas aiding buoyancy forces ($N > 0$) inhibit species diffusion in the boundary layer. A similar retort remained by Rawat and Bhargava [27] and also Partha *et al.* [42].

Table 1: Skin friction coefficient $\left(-f''(0)\right)$, Nusselt number $\left(-\theta(0)\right)$ and Sharehood number $\left(-\phi(0)\right)$ for different values of **Pr**

S.No.	Pr	$f''(0)$	$-\theta(0)$	$-\phi(0)$
1	1	0.9846	0.4245	0.1671
2	5	0.8601	0.7976	0.1028
3	10	0.8037	1.0425	0.0678
4	20	0.7456	1.3940	0.0208
5	50	0.6540	2.3823	-

Table 2: Skin friction coefficient $\left(-f''(0)\right)$, Nusselt number $\left(-\theta(0)\right)$ and Sharehood number $\left(-\phi(0)\right)$ for different values of **M**

S.No.	M	$f''(0)$	$-\theta(0)$	$-\phi(0)$
1	1	1.0087	0.3677	0.1797
2	5	0.6275	0.2517	0.1155
3	10	0.4691	0.1934	0.0901
4	15	0.3904	0.1627	0.0789
5	20	0.3413	0.1431	0.0727

Figures 7(a)–7(c) depict the velocity $f'(\eta)$, temperature $\theta(\eta)$ and concentration $\phi(\eta)$ distributions for various values of Prandtl number Pr. It is observed that an increase in the Prandtl number significantly decelerates the flow i.e., velocity and temperature decreases. Also, increasing Prandtl number is found to upturns the concentration.

Table 3: Values of the local heat transfer coefficient (Nu) for various values of ξ

ξ	$-\theta'(\xi,0)$		
	Yih	Merkin	Present
0.0	0.4241	0.4241	0.4241
0.4	0.4184	0.4182	0.4283
0.8	0.4096	0.4093	0.4095
1.2	0.3950	0.3942	0.3951
1.6	0.3740	0.3727	0.3745
2.0	0.3457	0.3443	0.4351
2.4	0.3086	0.3073	0.3088
2.8	0.2595	0.2581	0.2592
π	0.1962	0.1963	0.1962

Figures 8(a)-8(c) depict the velocity $f'(\eta)$, temperature $\theta(\eta)$ and concentration $\phi(\eta)$ distributions for different values of Schmidt number Sc. It is observed that increases in Schmidt number significantly decelerates the flow i.e., velocity and concentration decreases. Also increases the Schmidt number is found that upturns the temperature.

Figures 9(a)-9(b) the combined effect of Dufour number $\left(Du\right)$ and Soret number $\left(Sr\right)$ on the temperature and concentration distributions, respectively, in the regime are shown. We study the simultaneous increase (and decrease) of these parameters so that their product remains constant at 0.05, following Beg *et al.* [23]. Increasing Dufour number causes a rise in temperature whereas an increase in Soret number cools the fluid *i.e.* reduces temperature, as observed in Figure 9(a). Conversely in Figure 9(b), we observe that a rise in *Du* decreases the concentration values in the boundary layer, whereas a rise in Soret number increases values.

5. CONCLUSION

The objective of the present paper is to investigate the steady boundary-layer MHD flow and heat transfer of Eyring Powell fluid past a horizontal circular cylinder in a non-Darcy porous medium. Mathematical modeling through equations of continuity and motion leads to a nonlinear differential equation even after employing the boundary layer assumptions. The present study has to the authors knowledge not appeared thus far in the scientific literature. Numerical solutions have been presented for the heat transfer of Eyring-Powell flow external to a horizontal cylinder. The Keller-box implicit second order accurate numerical scheme has been utilized to efficiently solve the transformed, dimensionless velocity and boundary layer equations, subject to realistic boundary conditions. Excellent correlation with previous studies has been demonstrated testifying to the validity of the present code. The computations have shown that:

1. Increasing Eyring-Powell fluid parameter (ε), reduces the velocity and skin friction and heat transfer rate, where it elevates temperatures in the boundary layer.
2. Increasing local non-Newtonian parameter (δ), increases the velocity, skin friction and Nusselt number for all values of tangential coordinate(ξ) i.e., throughout the boundary layer regime whereas it depresses temperature.
3. Increasing Prandtl number (Pr), decreases velocity and temperature.

REFERENCES

1. Livescu, S., Mathematical modeling of thixotropic drilling mud and crude oil flow in wells and pipelines—A review, *J. Petroleum Science and Engineering*, 2012, 98/99, 174–184.
2. Hron, J., Málek, J., Pustějovská, P. and Rajagopal, K.R., On the modeling of the synovial fluid, *Advances in Tribology*, 2000, Volume 2010 , Article ID 104957, 12 pages. http://dx.doi.org/10.1155/2010/104957.
3. Loix, F., Orgéas, L., Geindreau,C., Badel, P., Boisse, P. and Bloch, J.F., Flow of non-Newtonian liquid polymers through deformed composites reinforcements, *Composites Science and Technology*, 2009, 69, 612–619.
4. Viviane Kechichian, Gabriel P. Crivellari, Jorge A.W. Gut, Carmen C. Tadini, Modeling of continuous thermal processing of a non-Newtonian liquid food under diffusive laminar flow in a tubular system, *Int. J. Heat and Mass Transfer*,2012, 55, 5783–5792.
5. Malik.M.Y, et al, Mixed convection flow of MHD Eyring-Powell nanofluid over a stretching sheet a numerical study *AIP advances* 2015, **5** 117118.
6. Abdul Gaffar.S, Ramachandra Prasad.V ,Keshava Reddy. E, computational study of non-Newtonian eyring-powell fluid from a horizontal circular cylinder with biot number effects *International Journal of Mathematical Archive* 2015, **6(9)** 114-132.
7. Hayder Ibrahim Mohammed et al, Comparison between Two Vertical Enclosures Filled With Porous Media under the Effect of Radiation and Magneto hydrodynamics *Journal of Energy and Power Engineering* 2013, **7,** 37-49.
8. Rashidi. M.M, Mohamed et al, Entropy Generation on MHD Casson Nano fluid Flow over a Porous Stretching/Shrinking Surface *Entropy*, 2016, 18 12.
9. Abdul Hakeema. A.K, Vishnu Ganesha.N Gangab.B, Heat transfer of non-Darcy MHD flow of nano-fluid over a stretching/shrinking surface in a thermally stratified medium with second order slip model *Scientia Iranica F*, 2015, **22(6)** 2766-2784.
10. Animasaun.I.L,. Raju.C.S.K, Sandeep.N, Unequal diffusivities case of homogeneous–heterogeneous reactions within viscoelastic fluid flow in the presence of induced magnetic-field and nonlinear thermal radiation *Alexandria Engineering Journal* 2016, 55 1595–1606.
11. Subba Rao. A, Ramachandra Prasad.V, Nagendra.N, Bhaskar Reddy.N and Anwar Beg.O, Non-Similar Computational Solution for Boundary Layer Flows of Non-Newtonian Fluid from an Inclined Plate with Thermal Slip *Journal of Applied Fluid Mechanics* 2016, **2**, 795-807.
12. Keller, H.B., Numerical methods in boundary-layer theory, *Ann. Rev. Fluid Mech*. 1978, 10, 417-433.
13. Subhas Abel, M., Datti, P.S., Mahesha, N., Flow and heat transfer in a power-law fluid over a stretching sheet with variable thermal conductivity and non-uniform heat source,*Int. J. Heat Mass Transfer 2009*, 52, 2902-2913.
14. Vajravelu, K., Prasad, K.V., *et. al*, Convective heat transfer in the flow of viscous Ag–water and Cu–water nanofluids over a stretching surface, *Int. J. Thermal Sciences*, 2011, 50, 843-851.
15. Chen,C.H., Magneto-hydrodynamic mixed convection of a power-law fluid past a stretching surface in the presence of thermal radiation and internal heat generation/absorption, *Int. J. Non-Linear Mechanics*, 2009, 44, 596-603.
16. Zhangand, Y.L., Vairavamoorthy, K., Analysis of transient flow in pipelines with fluid–structure interaction using method of lines, *Int. J. Num. Meth. Eng*, 2005, 63, 1446-1460.
17. OrhanAydın and Ahmet Kaya, Non-Darcian forced convection flow of viscous dissipating fluid over a flat plate embedded in a porous medium, *Transport in Porous Media*, 2008, 73, 173-186.
18. Kumari, M., Nath,G., Steady mixed convection stagnation-point flow of upper convected Maxwell fluids with magnetic field, *Int. J. Nonlinear Mechanics*, 2009, 44, 1048-1055.

19. Yih, K.A., Viscous and Joule Heating effects on non-Darcy MHD natural convection flow over a permeable sphere in porous media with internal heat generation, International Communications in Heat and mass Transfer, 2000, 27(4), 591-600.
20. Rawat. S., Bhargava, R., "Finite Element Study of Natural Convective Heat and Mass Transfer in a Micropolar Fluid-Saturated Porous Regime with Soret/Dufour Effects," International Journal of Applied Mathematics and Mechanics, 2009, 5, 2, 58-71.
21. Partha, M. K., Murthy, P. V. S. N., and Rajaskhar, G. P. "Soret and Dufour Effects in a Non-Darcy Porous Medium," ASME Journal of Heat Transfer, 2006, 128, 6, 605-610.
22. Osman Anwar Beg, Ahmed Bakier, Ramachandra Prasad, Swapan Kumar, Numerical Modelling of Non-Similar Mixed Convection Heat and Species Transfer along an Inclined Solar Energy Collector Surface with Cross Diffusion Effects. World Journal of Mechanics, 2011, 1, 185-196.
23. Merkin JH. Free convection boundary layers on cylinders of elliptic cross section. J. Heat Transfer 1977; 99: 453–457.
24. Yih KA. Effect of blowing/suction on MHD-natural convection over horizontal cylinder: UWT or UHF. Acta Mech 2000; 144: 17–27.
25. Eswara. A.T. and Nath G., 1992, Unsteady forced convection laminar boundary layer floe over a moving longitude cylinder. Acta. Mech., 93.
26. Rotte, J.W. and Beek, W,J., 1969, Some models for the calculation of heat transfer coefficients to moving continuous cylinder. Chem. Eng. Sci., 24, 705-716.
27. Sakidas, B.C, 1961, Boundary behavior on continuous solid surface, III The boundary layer on a continuous cylindrical surface. AIChE. J., 7:467-472.
28. Zueco, J., Anwar Beg, Tasveer A. Beg and Takhar. H.S., 2009, Numerical study of chemical reactive buoyancy-driven heat and mass transfer across horizontal cylinder in a high porosity non-Darcian regime, J. of porous media, 12, 519-535.
29. Subba Rao. A, V.R.Prasad, K. Harshavalli and O. Anwar Bég, Thermal radiation effects on non- Newtonian fluid in a variable porosity regime with partial slip, J. Porous Media, 19(4) (2016) 313-329.
30. Subba Rao A, Prasad V.R, Nagendra N, Murthy K.V.N, Reddy N.B and Beg O.A (2015) Numerical Modeling of Non-Similar Mixed Convection Heat Transfer over a Stretching Surface with Slip Conditions. World Journal of Mechanics, 5,117- 128.
31. Subba Rao. A, N. Nagendra " Thermal Radiation Effects on Oldroyd-B Nano fluid from a Stretching Sheet in a non- Darcy porous medium" Global Journal of Pure and Applied Mathematics, Vol.11, No.2, pp.45-49(2015).
32. Subba Rao. A, V.R. Prasad, N. Bhaskar Reddy, O. Anwar Beg, Modelling Laminar Transport Phenomena in a Casson rheological fluid from a Semi-Infinite Vertical Plate with Partial Slip; Heat Transfer-Asian Research vol. 44, No. 3, pp. 272-291(2015) DOI: 10.1002/htj.21115
33. Subba Rao. A, V.R. Prasad, N. Bhaskar Reddy and O. Anwar Beg, Modelling Laminar Transport Phenomena In A Casson Rheological Fluid From An Isothermal Sphere With Partial Slip, (2015); Thermal science, Vol. 19, No.5, pp. 1507-1519; doi:10.2298/TSCI120828098S
34. V. Ramachandra Prasad, A. Subba Rao, N. Bhasakar Reddy, B.Vasu and O. Anwar Beg, "Modelling Laminar Transport Phenomena in a Casson rheological fluid from a Horizontal Circular Cylinder with Partial Slip" I. Mech E. Journal of Process Engineering, Vol. 227 Issue 4 pp. 309-326 (2013); DOI: 10.1177/0954408912466350
35. Subba Rao. A, CH. Amanulla, N. Nagendra, O. Anwar Beg and A. Kadir (2017), Hydromagnetic Flow And Heat Transfer In A Williamson Non-Newtonian Fluid From A Horizontal Circular Cylinder With Newtonian Heating; International Journal of Applied & Computational Mathematics – Springer; DOI 10.1007/s40819-017-0304-x
36. Subba Rao. A, V. R. Prasad and O. Anwar Beg , Computational analysis of Viscous Dissipation and Joule-Heating effects on non-Darcy MHD natural convection flow from a Horizontal Cylinder in Porous Media with Internal Heat Generation, Theoretical and Applied Mechanics. TEOPM7, Vol.41, No.1, pp.37-70, (2014). doi:10.2298/TAM1401037P
37. V. Ramachandra Prasad, A. Subba Rao and O. Anwar Beg, Flow and Heat Transfer of non-Newtonian Casson fluid from an Isothermal Sphere with Partial Slip in a non-Darcy Porous Medium, Theoretical and Applied Mechanics, Vol 40, Issue 4, pp.469-510(2013); doi:10.2298/TAM1303465P
38. V. Ramachandra Prasad, A. Subba Rao and O. Anwar Beg, Flow and Heat Transfer of Casson fluid from a Horizontal Circular Cylinder with Partial Slip in non-Darcy Porous Medium; Journal of Applied & Computational Mathematics, ISSN: 2168-9679; Volume 2 • Issue 3 • 1000127 (2013); http://dx.doi.org/10.4172/2168-9679.1000127
39. A Subba Rao, N Nagendra, V. Ramachandra Prasad. (2015) Heat Transfer in a Non-Newtonian Jeffery's Fluid over a Non-Isothermal Wedge, Procedia Engineering, 127,775-782.
40. Zueco, J., Anwar Beg, H.S. Takhar and Nath, G., 2011, Network simulation of laminar convective heat and mass transfer over a vertical slender cylinder with uniform surface heat and mass flux, J. of applied fluid mechanics, 4, 13-23.

41. Chen S.S and Leonard R., 1972, The axisymmetric boundary layer for a power-law non-Newtonian fluid on a slender cylinder, Chem. Eng. J., 3,88-92.
42. Anwar. O., Zueco, B.J., Bhargava. R., Takhar, H.S., 2009, Magnetohydrodynamic convection flow from a sphere to a non-Darcian porous medium with heat generation or absorption effects: network simulation, Int. J. Thermal Sci. 48 913-921.

Source of support: Nil, Conflict of interest: None Declared.